Eur Biophys J (2006) 35: 92–103
DOI 10.1007/s00249-005-0007-9

REVIEW

Miguel A.R.B. Castanho · Miguel X. Fernandes

Lipid membrane-induced optimization for ligand–receptor docking: recent tools and insights for the "membrane catalysis" model

Received: 18 May 2005 / Revised: 7 July 2005 / Accepted: 18 July 2005 / Published online: 11 October 2005

Abstract Cells in living organisms are regulated by chemical and physical stimuli from their environment. Often, ligands interact with membrane receptors to trigger responses and Sargent and Schwyzer conceived a model to describe this process, "membrane catalysis". There is a notion that the physical organization of membranes can control the response of cells by speeding up reactions. We revisit the "membrane catalysis" model in the light of recent technical, methodological and theoretical advances and how they can be exploited to highlight the details of membrane mediated ligand–receptor interactions. We examine the possible effects that ligand concentration causes in the membrane catalysis and focus our attention in techniques used to determine the partition constant. The hypothetical diffusional advantage associated with membrane catalysis is discussed and the applicability of existing models is assessed. The role of in-depth location and orientation of ligands is explored emphasizing the contribution of new analysis methods and spectroscopic techniques. Results suggest that membranes can optimize the interaction between ligands and receptors through several different effects but the relative contribution of each must be carefully investigated. We certainly hope that the conjugation of the methodological and technical advances here reported will revive the interest in the membrane catalysis model.

Keywords Receptor · Ligand · Membrane · Dichroism · Quenching · Diffusion

Miguel A.R.B. Castanho (✉)
Centro de Quìmica e Bioquímica, Faculdade de Ciências da Universidade de Lisboa, Campo Grande Ed. C8, 1749-016 Lisboa, Portugal
E-mail: castanho@fc.ul.pt
Fax: +351-21-7500088

Miguel X. Fernandes
Centro de Química da Madeira, Departamento de Química, Universidade da Madeira, Campus da Penteada, 9000-390 Funchal, Portugal

Abbreviations IRE: Internal reflection element · POPC: 1-Palmitoyl-2-oleoyl-*sn*-glycero-3-phosphatidyl choline · RD: Reduction of dimensionality

Introduction

Twenty years ago D.F. Sargent and R. Schwyzer published a paper where they conceived a model for membrane-mediated peptide–receptor interaction (Sargent and Schwyzer 1986), referred to as "membrane catalysis", evoking the reminiscent similarities with micelle-catalyzed chemical reactions. By then, the group of R. Schwyzer had collected evidence that several peptide ligands interact strongly and specifically with pure lipid bilayers, with local, conformational and orientational constraints resulting there from. The concept behind the model had a high impact in the work developed by others and became an historical landmark in the growing field of peptide–membrane–receptor interaction. In 1995, the model applications were reviewed (Schwyzer 1995a). Recent advantages in the methodologies that enable additional insights into peptide–membrane interaction, mainly in membrane in-depth location and orientation of peptides prompted us to review the most recent tools that can be used to refine the model. Although this paper focuses mainly on methodologies and techniques, the largely unexplored topic of hypothetical diffusional advantage associated with the model will be addressed.

Although the matters dealt with in this paper will be presented in the context of the "membrane catalysis" model, they can be used to study a wide range of membrane-related phenomena, including a number of peptide–membrane interaction events (Fig. 1). As Sargent and Schwyzer wrote in a premonitory sentence: "[Molecular] Interactions with the lipid phase, be they at the interface or in the hydrophobic core, are probably more widespread than has been realized." (Sargent and Schwyzer 1986).

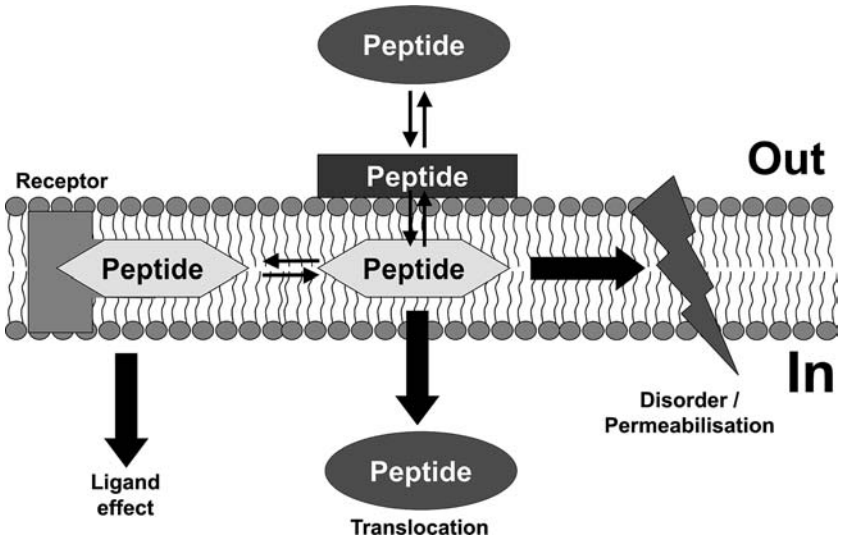

Fig. 1 Outline of peptide–membrane interactions. Peptides in contact with membranes may change conformation, which may facilitate proper binding to a receptor. Peptides may also exert local specific effects like disorder and permeabilization (e.g. AMPs, antimicrobial peptides). Other peptides have the ability to translocate through the membrane, having no apparent effect in the lipid bilayer

The "membrane catalysis" model

The "membrane catalysis" model relies on evidence that a certain receptor of interest, R, specific for a certain ligand, L, occupy only a small fraction of the total cell surface, so that when L approaches a cell the first contact is much more likely to be with the lipid phase than with one of its own receptors. Considering that upon insertion of L in membranes the local concentration increases and the molecule may acquire conformational constraints that favour L/R docking, the receptor will bind predominantly membrane-associated ligands rather than those free in solution.

A quantitative formalism can be constructed from a simple phenomenological three-step model (Fig. 2):

Step 1: Membrane adsorption/electrostatic accumulation

The Boltzmann distribution can account for the electrostatic accumulation of L at the membrane surface:

$$[\mathrm{L}]_\mathrm{a} = [\mathrm{L}]_\mathrm{w} \exp(-z_\mathrm{L} FV/RT), \tag{1}$$

where $[\mathrm{L}]_\mathrm{a}$ is the ligand concentration at the accumulation layer, $[\mathrm{L}]_\mathrm{w}$ the free ligand concentration in solution, V the surface potential, z_L the ligand charge, F the Faraday constant, and T temperature.

Step 2: Membrane effective binding

Sargent and Schwyzer considered the following equilibrium to account for the insertion of the ligand in the lipid matrix (step 2 in Fig. 2):

$$\mathrm{L_a} + \mathrm{B_m} \leftrightarrows \mathrm{LB_m}, \tag{2}$$

where $\mathrm{B_m}$ is a surface membrane binding site and $\mathrm{LB_m}$ the "surface-bound" ligand. Defining k^+ and k^- as the forward and reverse rate constants for reaction (2), then

$$[\mathrm{LB_m}] = \frac{[\mathrm{B}]_0}{1 + k^-/(k^+[\mathrm{L_a}])} \tag{3}$$

where $[\mathrm{B}]_0$ is the total binding sites concentration. $k^-/k^+ = \exp(\Delta G_\mathrm{m}/RT)$, where ΔG_m is the change in standard free energy for the membrane binding.

Step 3: Ligand–receptor docking

Again a simple molecular equilibrium is considered:

$$\mathrm{LB_m} + \mathrm{R} \leftrightarrows \mathrm{LR} + \mathrm{B_m}. \tag{4}$$

Defining rate constants, k^+ and k^-, total receptor concentration, $[\mathrm{R}]_0$, and the change in standard free energy upon docking $\Delta G_\mathrm{r} = RT \ln (k^- / k^+)$, and substituting for $[\mathrm{LB_m}]$ and $[L_\mathrm{a}]$,

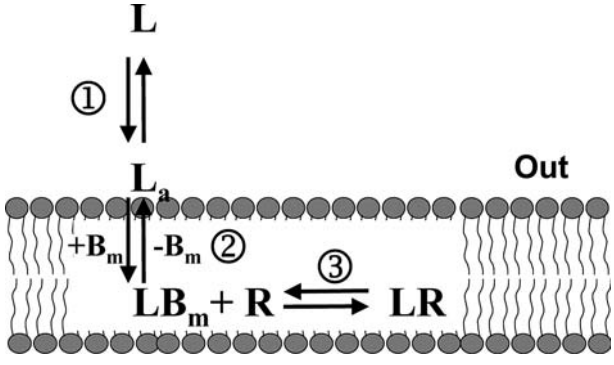

Fig. 2 Brief description of the three-step "membrane catalysis" model. 1: adsorption of the ligand L to the membrane and formation of an accumulation layer (L_a); 2: insertion in the membrane at specific binding sites (B_m); 3: receptor (R) docking in the membrane matrix

$$[\mathrm{LR}] = \frac{[R]_0}{1 + [L]_\mathrm{W}^{-1} \exp\left[(\Delta G_\mathrm{m} + \Delta G_\mathrm{r} + z_\mathrm{L} F V)/RT\right]} = \frac{[R]_0}{1 + [L]_\mathrm{W}^{-1} \exp\left[\Delta G^0_\mathrm{exp}/RT\right]}, \quad (5)$$

where $\Delta G^0{}_\mathrm{exp}$ (measured) is related to the apparent global dissociation constant, $K_\mathrm{d,app}$, of LR: $\Delta G^0{}_\mathrm{exp} = RT \ln (K_\mathrm{d,app})$.

Models that are widely used to describe peptide–lipids interactions nowadays still use the concepts of steps 1 and 2 (Murray et al. 2002). From the reaction kinetics point of view, a combined two-step mechanism is very important because the membrane insertion step is rate limiting and the reaction kinetics will be some 10^5 times faster than for the single-step process without electrostatic accumulation (Sargent and Schwyzer 1986). Even for electrically neutral, membrane-mediated ligand–receptor interaction, there is kinetic advantage because a significant increase in the overall reaction rate is obtained compared to a single-step reaction with an equivalent total ΔG.

Receptor docking (third step) needs only a small energetic contribution. The binding energy between the peptide and the membrane is utilized to overcome the entropy requirements involved in bringing aqueous L and R together.

In spite of its soundness, the membrane catalysis model has two formulation weaknesses that do not jeopardize its application but are important to consider: (1) the receptor docking site in the model is assumed to be in the lipid environment, which is frequently hard to prove and (2) membrane binding sites $\mathrm{B_m}$ have no physical counterpart. A more realistic option would be to consider equilibrium 2 as a partition phenomenon, therefore described by a partition constant, K_p (Santos et al. 2003), which in this case would read:

$$K_\mathrm{p} = [\mathrm{L_m}]_\mathrm{m}/[\mathrm{L_a}]_\mathrm{a}, \quad (6)$$

where $[\mathrm{S}]_\mathrm{i}$ refers to the concentration of species S ($\mathrm{S} = \mathrm{L_m}$ or $\mathrm{S} = \mathrm{L_a}$) in the volume of environment i (membrane, $\mathrm{i} = \mathrm{m}$, or accumulation layer, $\mathrm{i} = \mathrm{a}$).

Is there a diffusional advantage associated with the model?

An eventual advantage relating to the reduction of dimensionality from 3D to 2D was barely explored by Sargent and Schwyzer. However, Adam and Delbrück (1968) theorized that reaction rates between ligands and surface bound receptors would be increased by non-specific ligand adsorption and 2D diffusion towards receptors. This effect is referred to as reduction of dimensionality (RD) reaction rate enhancement. Since then, several theoretical models attempted to describe the relevance of underlying factors to this behaviour (DeLisi 1980; Cukier 1983; Gershon et al. 1985; Erickson et al. 1987; Baldo et al. 1991). However, as justly referred by Martins et al. (2004) caution must be exerted when comparing a 2D reaction with a 3D counterpart, namely not disregarding the clause "other factors being equal". When going from 3D to 2D some factors will face changes inherent to the reduction of dimensionality, as it happens with the diffusion coefficient. Nonetheless, other factors regarding the presence of ligands and receptors can be kept unaltered. For instance, the total number of receptors, the fractional area/volume occupied by them or their concentration can be held fixed, and the same applies to ligand-related parameters.

All models derived to study the RD enhancement involve the participation of several different factors, namely the 2D and 3D diffusion coefficients, k^+ and k^- rates, the concentration of receptors, curvature of the membrane, thickness of the membrane or even shape of the receptor. Not all the models use every parameter described above, but the results for RD enhancement vary greatly depending upon the relative magnitude of the intervening parameters and for some specific conditions, not altogether unrealistic, there is no RD advantage and the opposite effect takes place.

Haugh and Lauffenburger (1997) derive expressions for several alternative mechanisms of membrane receptor activation, and using order of magnitude reasoning they arrive at an enhancement factor of 10^2–10^3 when moving from 3D to 2D, for reaction-limited processes (the rate limiting step is not diffusion). The enhancement factor reflects the reduction of the sampling volume and is equivalent to the ratio between the volume of a membrane when compared to the volume of a cell.

One of the most complete analyses about reversible binding receptors is presented by Axelrod and Wang (1994). They show that the RD enhancement for reaction-limited processes depend strongly on the reaction probability and on the magnitude of the 2D diffusion coefficient. For instance, when one has a reaction probability of 0.001, both in 2D and 3D, the RD enhancement goes from 1.5 to 337 when the 2D diffusion coefficient changes from 10^{-9} to 10^{-6} $\mathrm{cm^2/s}$, respectively. This strong dependence on parameter values and molecular details, advises us to restrain the claims of RD advantage.

This section is devoted to the diffusional advantage and though the results reported above were for the case of reaction-limited processes, they depended on the diffusion coefficients to some extent. For the case of diffusion-limited processes (diffusion is the rate limiting step), with irreversible binding receptors (meaning that the ligand instantly disappears when it binds the receptor), Martins et al. (2004) arrived at the expression

$$\frac{t_2(N_2)}{t_3(N_3)} = 1.5 \frac{D_3 N_3 a}{D_2 N_2 b} \ln\left(\frac{b}{a\sqrt{N_2}}\right). \quad (7)$$

This equation allows the quantification of the RD enhancement factor. The subscripts 2 and 3 refer to the dimensionality (2D and 3D, respectively) and a ratio value bigger than one implies a RD disadvantage.

Regarding the parameters, t is the mean lifetime of a ligand before it reaches a receptor, N the number of receptors, D the diffusion coefficient, a the radius of the receptor and b the radius of the surface/sphere. The equation explicitly shows the dependence of the mean lifetimes on the number of receptors. Martins et al. (2004) use 3 different options to ensure that all other factors do not influence the outcome of the ratio. In the first option they make $N_2 = N_3$, meaning we have the same absolute number of receptors in 2D and 3D and the value of the ratio will depend on the relative magnitudes of D_3 and D_2 (D_3 is generally 10^2–10^3 times greater than D_2), the relative magnitudes of a and b (b is generally 10^3 times bigger that a) and on the absolute value of N_2. The second option sets $N_2 b = N_3 a$, which is equivalent to say that the receptors occupy the same fraction of available space in 2D and 3D. The third option sets $N_3/N_2 = \sqrt{N_2}$, which means that the average distance between the receptors in 2D and 3D is the same. Perhaps this last option is the most plausible for biological systems, and in a case where $b = 1$ μm, $a = 1$ nm and $D_3 = 100 D_2$, there is no RD advantage, in fact there is a disadvantage that increases with increasing number of receptors. For the first and second options, we get a RD disadvantage choosing normally accepted values for the parameters intervening in Eq. (7).

With the vast number of possibilities compiled here one can say that there is RD enhancement in most cases for reaction-limited processes (in a very strict sense they would fall in the situations tackled in the other sections of this paper). For diffusion-limited processes there is a disadvantage in conditions plausible to occur in biological systems. Therefore, a thoughtful analysis of each system should be performed in order to model it appropriately if a RD advantage is to be foreseen.

The concentration advantage: quantifying partition

The increased local concentration of the ligand in the vicinity of the receptor is one of the easiest advantages of membrane-mediated interaction to illustrate and quantify. While electrostatic accumulation is important to show that receptor-binding kinetics may be 10^5 times faster than in its absence (Sargent and Schwyzer 1986), steady-state considerations can be made clearer considering the bulk aqueous medium versus membrane concentration balance. Figure 3 outlines the equilibria involved in membrane-mediated ligand–receptor docking in a more simplified way than the membrane catalysis model because membrane insertion is accounted for in a single step and no membrane binding sites are evoked. Combining the partition constant equation applied to this case, $K_p = [L_m]_m/[L_w]_w$, with the equilibrium constant for ligand–receptor binding, $K_b = [LR]_m/([LB_m]_m[R]_m)$, the occupied-to-unoccupied receptor binding sites molar ratio is

$$\frac{[LR]_m}{[R]_m} = \frac{n_{LR}}{n_R} = K_p K_b [L_w]_w. \tag{8}$$

In the absence of the lipid membrane, the ligand–receptor interaction in homogenous medium would lead to $n_{LR}/n_R = K_b[L_w]_w$. Therefore, the concentrating effect of the membrane is expected to increase the occupied-to-unoccupied receptor binding sites ratio by a K_p factor. Typical moderate values of K_p are 10^3–10^4 in the absence of electrostatic attraction and 10^5–10^6 when electrostatic attraction is present (Henriques and Castanho 2004; Veiga et al. 2004a, 2004b). Thus, membrane intermediation can improve the extent of ligand–receptor binding up to several orders of magnitude.

K_p can be calculated in lipid vesicles of controlled composition to mimic cell membranes. Large unilamellar vesicles (LUV) are commonly used because (1) being unilamellar there is quantitative exposure of the lipid to molecules added to the bulk aqueous medium, and (2) being large, no curvature effects bias both molecular partition and location in the lipid matrix. The total quantity of the solute in the sample is usually known; therefore, the practical task in K_p determination is to quantify the fraction of the solute in one of the phases (lipid or aqueous). Two major classes of methodologies exist for this purpose (Santos et al. 2003) depending on whether there is a demand for the physical separation of free and membrane-bound molecules or not. The first involves mostly spectroscopic approaches. Several spectroscopic signals are a balance between the signals originated from the molecules located in both phases, the balance depending on the fractional distribution of the molecules between aqueous and lipid media, i.e. on K_p. In the absence of effects other than partition that can interfere with the measured spectroscopic parameter, p, its dependence on the lipid concentration, $[lip]_w$, is expected to be

$$p = \frac{p_w + K_p \gamma_m [lip]_w p_m}{1 + K_p \gamma_m [lip]_w} \tag{9}$$

assuming $\gamma_m [lip]_w \ll 1$ (i.e. a small fractional volume of the lipid), a condition attained in most experiments using vesicles suspensions. p may stand for electronic absorbance, fluorescence intensity, the fluorescence

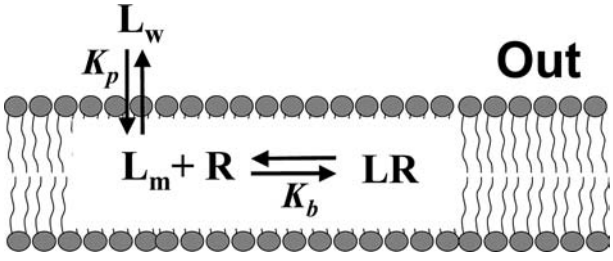

Fig. 3 Simplified scheme for the membrane catalysis model, where no membrane binding sites are considered and partition is described by a single equilibrium step. K_p and K_b are equilibrium constants for partition into the membrane and binding to receptor, respectively (L_i refers to ligand L in location i—bulk aqueous phase, i = w, or membrane, i = m)

lifetime-weighted quantum yield, or the fluorescence steady-state anisotropy (provided that the absorptivity × quantum yield product does not change upon membrane insertion; Santos et al. 2003), or any other additive spectroscopic parameter. p_i is the signal that would be obtained if all the solute molecules were in environment i (membrane, i = m, or aqueous, i = w), γ_m is the molar volume of the lipid and $[lip]_w$ the molar concentration of the lipid. The expected variation of p upon titration of the solute with lipid is outlined in Fig. 4a. Figures 4b and c illustrate the application limits of Eq. (9). K_p can be obtained from non-linear regression fit of Eq. (9) to experimental data. This methodology relies on the assumption that the limit of saturation of the membrane by the solute is not achieved, which may be critical at low lipid concentrations when K_p is very high. In this case a new partition formalism needs to be derived (M. Melo et al. 2005, unpublished results). Even in the absence of saturation, the local concentration of the solute in the membrane at low lipid concentration may be high enough for the occurrence of concentration-dependent phenomena that may interfere with the experimental signal. Self-quenching, for instance, may interfere when fluorescence intensity is the chosen spectroscopic parameter. In this case, the formalism has to be adapted to account for simultaneous self-quenching and partition, a more complex equation than Eq. (9) being obtained (Henriques and Castanho 2005). At variance, phase coexistence in membranes does not require a revision of the formalism: the partition coefficient between different lipid phases is simply the ratio of their individual partition coefficients, measured when phases are used separately in different samples (Castanho and Prieto 1992; Santos et al. 2003).

If no physical (spectroscopic) signal is generated in the sample, one needs to separate aqueous and lipid phases in order to quantify free and membrane-bound solute molecules. Centrifugation, dialysis, filtration and chromatography techniques are among the most commonly used for that purpose (Santos et al. 2003). The main potential artefacts associated to some of these approaches are related to the incomplete separation of the phases and equilibrium perturbation during manipulation of the samples. Isothermal titration calorimetry (ITC) can also be used to calculate partition parameters (Høyrup et al. 2001). In chromatographic techniques, monolayers of phospholipids or phospholipid analogues are covalentely bonded to the hydrophobic end of the surface of silica particles and used as stationary phase in

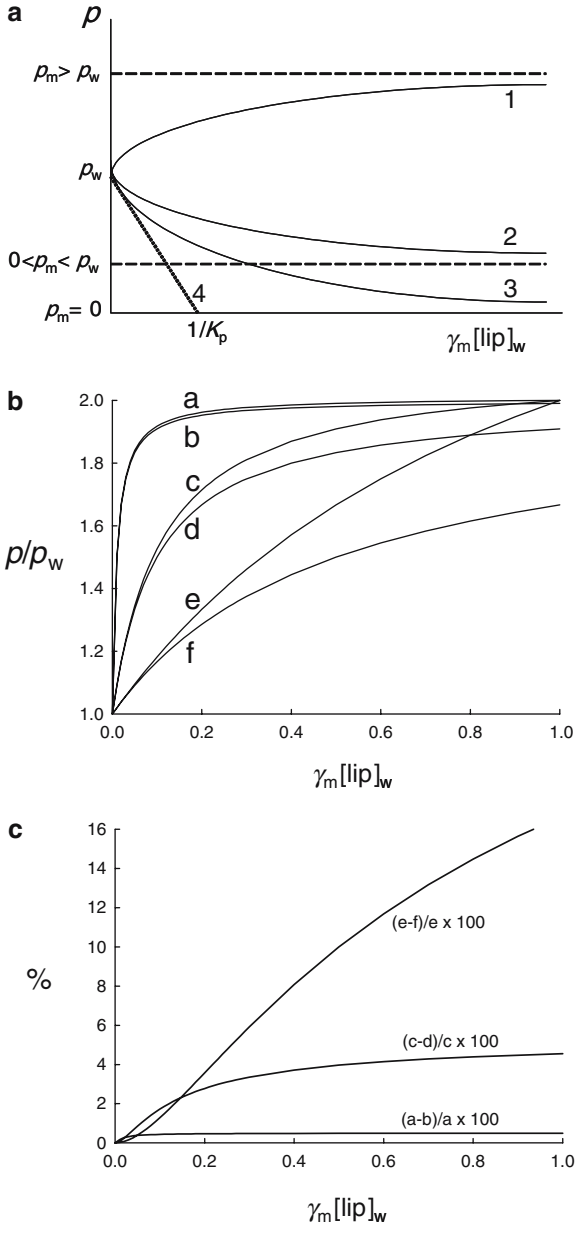

◀

Fig. 4 Panel **a** shows the type of dependence expected when an additive parameter p (electronic absorbance, fluorescence intensity, etc.) is followed during titration of a solute with lipid vesicles. $\gamma_m[lip]_w$ is an a dimensional variable, which is within the range [0,1]. However, in most experimental conditions the water content of the sample is very high and $\gamma_m[lip]_w \ll 1$. p_m (hypothetic p value that would be measured in the limit of having totally dehydrated lamellar bilayers) can be either bigger (curve 1) or smaller (curve 2) than p_w (p measured in the absence of the lipid). In the special case $p_m = 0$ (curve 3) K_p can be obtained from the slope of the initial regime of curve 3 (curve 4). Otherwise, K_p cannot be known without an estimate of p_m. Both K_p and p_m may be obtained from non-linear regression curve fitting. Equation (9) (see text) can be used to fit to experimental data. Although this equation is an approximation valid only for $\gamma_m[lip]_w \ll 1$, comparison of the simulated results in panel **b** for the exact (Santos et al. 2003) and approximate equation shows that the deviation (panel **c**) is negligible in all ranges of $\gamma_m[lip]_w$ when high values of K_p are involved. Even values as small as $K_p = 100$ lead to very similar results using the exact (curve a) and approximate (curve b) equations. The deviation is less than 1% from the exact solution (panel **c**). When the K_p is decreased to 10 (curve c obtained with exact equation and curve d obtained with approximate equation in panel **b**) or 2 (curve e obtained with exact equation and curve f obtained with approximate equation in panel **b**) the deviation increases and the approximated equation can only be considered a good alternative to the exact solution for $\gamma_m[lip]_w < 0.05$

liquid chromatography (Santos et al. 2003 and references therein).

The partition coefficient does not contain information other than the extent of solute distribution to lipid membranes. If structural, topographic or topological information relative to the solute present in the membrane is aimed, other experiments are needed.

The exposure control advantage: in-depth levelling of the ligand

Sargent and Schwyzer (1986) did not explicitly address the issue of the role of the membrane in positioning the ligand at the proper depth for receptor interaction. However, this issue cannot be ignored because the power of membranes to concentrate the ligand is not effective for docking unless receptor binding site and ligand are located at the same depth in the membrane. While the in-depth location of the binding site of receptors remains a difficult task, there are at present several methods to tackle the problem when smaller molecules like peptides are involved. The most common techniques used are spectroscopic and rely on the signal originated from reporter groups (fluorophores, spin labels, NMR-active nucleus, etc.) located along the lipid bilayer, from the interface to the inner core, and usually covalently attached to carbon atoms of the acyl chains of fatty acids or phospholipids in different positions. If this signal is somehow affected when the probe is in the vicinity of the solute, it is possible to infer on the location of the probe. Maximal interaction with the probe at depth z in the membrane, indicates the solute is near depth z. If the solute is fluorescent, such as Trp-, Tyr- and Phe-containing peptides or is fluorescently labelled, it is possible to use the differential quenching approach: being a contact interaction, collisional quenching is optimized when both fluorophore and quencher are buried at the same level in the membrane. Fluorescence quenching methodologies have two main advantages over other spectroscopic techniques such as NMR and EPR: (1) it is possible to use low concentrations of both fluorophore and quencher, and (2) the simplicity of the formalisms involved makes quantification much more appealing than with alternative techniques. Three main methods exist to estimate the depth or depth distribution of the fluorophores in the membrane. The Parallax Method (Chattopadhyay and London 1987) adapts the common simple methodology of the three-dimensional quenching sphere-of-action model to two dimensions. The underlying concept of static (non-diffusive) quenching (Castanho and Prieto, 1998) remains unchanged. This assumption confines the appropriate applicability of the model to few experimental cases, although it is often used without checking for this premise. The distribution analysis of depth-dependent fluorescent quenching ('distribution analysis', in short) was an alternative that overcame these limitations (Ladokhin 1997). It is a semi-empirical method built from the following assumptions: (1) the probability of quenching is proportional to the distance separating fluorophore and quencher, (2) a Gaussian function is adequate to describe the distribution of separating distances, and (3) the dynamics of the quencher during the excited state lifetime of the fluorophore is not dependent on its in-depth location (a controversial approximation, which may be reasonable in some conditions; Fernandes et al. 2002). Moreover, the quencher distribution width is considered constant, regardless of the quencher group position in the acyl chain. The mean locations of these distributions were obtained from pure brominated lipid bilayers and extrapolated to brominated lipids dispersed in bilayers of unlabelled lipids. Fluorophore distributions are obtained in a rather indirect way. To overcome some of the formal weaknesses of the parallax method, a third methodology was derived (Fernandes et al. 2002) applying the simple diffusional quenching concepts to the restricted dimensionality of a bilayer, which is treated as a slab where fluorophores and quenchers locate having a certain in-depth distribution. Single molecule Brownian Dynamics simulations were carried out to ascertain the quencher statistical location distributions. Pairs of quenchers (either brominated or doxyl-derivatized acyl chains in fatty acids or phospholipids) are then used to quench the fluorophore. The relative degree of quenching between them depends on the known distributions of the quenchers and on the yet unknown fluorophore distribution. The probability density function for the location of the fluorophore along the depth coordinate z, is assumed to be Lorentzian (a function that allies handling simplicity both in analytical and numerical methods to the advantages of a Gaussian-like distribution) and the problem consists in finding the centre and width of the distribution that simultaneously makes the theoretical expectation match the experimental

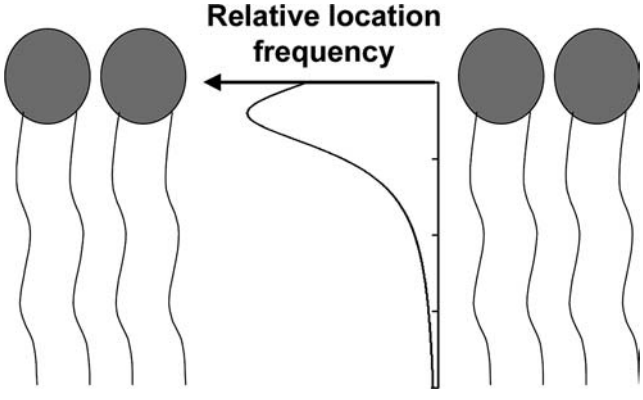

Fig. 5 Relative location frequency of the HIV fusion inhibitor peptide T20 (enfuvirtide) in POPC, obtained from differential fluorescence quenching methodologies. Fluorescence quenching with a pair of doxyl moieties attached to fatty acids at position 5 or 16 of the carbon chain (Fernandes et al. 2002) enables calculation of the in-depth location of the Trp residues of the peptide. The shallow location of the peptide in the mammalian cell membranes favours interaction of the peptide with the proteins of the viral envelope leading to virus/cell fusion inhibition (Veiga et al. 2004a, 2004b)

results for both quenchers. The computation is numerical, and the methodology was tested with a simple molecule, *trans*-parinaric acid. The methodology was recently applied to study the location of the HIV fusion-inhibitors T20 (enfuvirtide) and T1249, which were found to use membranes in the "catalytic" fashion similar to the one envisaged by Sargent and Schweizer (Veiga et al. 2004a, 2004b). A shallow average position of the Trp residues was concluded, which helps position the whole molecular ensemble in the lipid bilayer (Fig. 5).

The orientational advantage: constraining the orientational freedom of the ligand

Along with concentration and conformation modulation, the most important role of membranes in their "catalysis" is ligand orientation modulation. However, most of the work of R. Schwyzer is focused on the conformational issue and little factual importance is given to the experimental proof of orientation modulation. The ability of membranes to reduce the orientational randomness of ligands remained speculative to a large extent. Yet, the theoretical frameworks to derive analytical equations simple enough to gain generalized acceptance among researchers in other fields than theoretical biophysics had very important contributions in the last two decades, paralleled by the breakthrough of new techniques. The most common spectroscopic methods used to determine the orientation of foreign molecules in membranes were reviewed very recently (Lopes and Castanho 2005). These include IR spectroscopy, UV–Vis linear dichroism, time-resolved fluorescence anisotropy decays, Raman spectroscopy, surface plasmon resonance and NMR. Two classes of approaches may be considered: (1) those where only the average orientation relative to the bilayer normal is obtained and (2) those where an approximated orientation distribution relative to the bilayer normal (i.e. the probability associated to each angle ψ, between the molecular axis and the bilayer normal; Fig. 6) can be estimated.

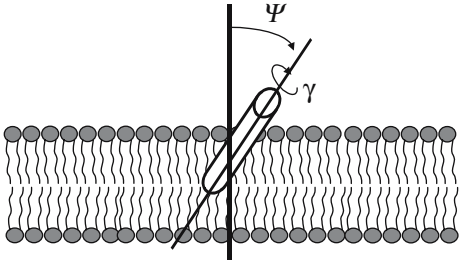

Fig. 6 Most spectroscopic techniques estimate either the average value of ψ or its probability density function. In NMR, ^{15}N chemical shifts of α-helical peptides in oriented membranes perpendicular to the magnetic field direction depend both on the molecular tilt angle (ψ) and rotational pitch angle (γ)

Average orientation calculation

Attenuated total internal reflection-Fourier transform infrared spectroscopy (ATR–FTIR) is one of the most popular methods to calculate average orientations and it has also been used to conclude on the average secondary structure of biologically important molecules (e.g. membrane proteins) inserted in lipid multibilayers (Axelsen and Citra 1996; Goormaghtigh et al. 1999; Tatulian 2003). A trapezoidal cell (internal reflection element, IRE), is covered with lipid multibilayers containing the molecule under study. These multibilayer films are obtained by applying an aqueous lipid suspension onto one side of the crystal and semi-drying it under a gentle stream of nitrogen. The infrared beam is then focused into the IRE and the light crosses the plate from one side to the other, by a series of internal reflections, originating an evanescent wave. The absorption of the energy of the resulting field by the lipids and other molecules inserted (e.g. proteins) generates the ATR–FTIR spectrum. In a macroscopically ordered deposited membrane on a solid support, as the ones used in ATR–FTIR experiments, every transition dipolar moment in the membrane molecules has the same average orientation relative to the normal of the IRE surface. Therefore, if one selects the orientation of the electric field component, by means of a polarizer, it is possible to detect the preferential orientation of the transition moment. Maximum or minimum light absorption will be observed, if the dipole transition moment is parallel or perpendicular to the electric fields component of the incident light, respectively. Detailed orientational information can be obtained by the calculus of the dichroic ratio:

$$R = \frac{A_{\parallel}}{A_{\perp}} \tag{10}$$

which is the ratio between the integrated absorption of a band measured with, a parallel and a perpendicular polarization of the incident light, respectively. This dichroic ratio is related to an orientational order parameter ($\langle P_2 \rangle$) :

$$R = a + b\left(1 + \frac{3\langle P_2 \rangle}{1 - \langle P_2 \rangle}\right) \tag{11}$$

in which

$$\langle P_2 \rangle = \frac{3\cos^2 \psi - 1}{2} \tag{12}$$

and where a and b depend on the time average square electric field amplitudes of the evanescent wave in the film at the IRE/film interface and ψ refers to the angle between the transition dipolar moment and the normal to the cell. Usually ATR–FTIR uses a combination of several characteristic bands to allow conclusions about the orientation and/or secondary structure (Heyse et al. 1998; Bechinger et al. 1999; Tatulian 2003). The dipole

transition moment is not always easily related to the molecular axis, however, and sometimes is necessary to combine ATR–FTIR studies with simulation studies in order to relate them (Lopes et al. 2004a). When one deals with α-helical peptides, the experimental $\langle P_2 \rangle$ is a product of three individual order parameters: (1) of the membrane with respect to the IRE, (2) of the helix within the membrane plane and (3) of the dipole orientation of amide I or amide II with respect to the helix axis (Goormaghtigh et al. 1999; Vigano et al. 2000).

Regardless of some limitations related to sample thickness determination and superimposition of vibrational bands, ATR–FTIR has three major advantages over other techniques: (1) light scattering problems are insignificant, (2) sometimes, depending on the molecules to be studied, it is possible to simultaneously study these molecules and lipids and (3) small sample volumes (~10 μl) are usually needed.

NMR has met important advancements in the domain of membrane-inserted peptide orientation recently (Zandomeneghi et al. 2001; Fung 2003; Wasniewski et al. 2004). Such advancements have been thoroughly reviewed by Bechinger et al. (2004). These authors consider the amide groups in peptides labelled with ^{15}N in such dilution that interactions between different labels are negligible and ^{1}H and ^{15}N nuclei to be decoupled. It is possible to relate the orientation of the tensor within the molecule with the magnetic field direction of the NMR spectrometer (laboratory macroscopic frame). The component of the chemical shift tensor projected in the magnetic field direction is related to the experimental NMR chemical shift value. Simulations of ^{15}N solid-state NMR obtained from a model for α-helical peptide reconstituted into oriented membranes with the membrane normal parallel to the magnetic field direction show progressive shifting of the resonance lines with varying patterns and broadness. The measured ^{15}N chemical shift is a function of both the tilt angle (ψ) and the rotational pitch angle (γ) as depicted in Fig. 6.

Estimation of the orientation distribution

The orientational distribution functions, $f(\psi)$ (Eq. 13), is related to Legendre polynomial series:

$$f(\psi) = \sum_{L\,\text{even}} \frac{1}{2}(2L+1)\langle P_L \rangle P_L(\cos\,\psi) \tag{13}$$

where $P_L(\cos\psi)$ are Legendre polynomials, $\langle P_L \rangle$ the ensemble-average of $P_L(\cos\psi)$ and is referred to as the Lth rank order parameter, when $L \neq 0$).

For an isotropic system, $\langle P_L \rangle = 0$ if $L \geq 2$ and $f(\psi) = 1/2$. For perfectly aligned molecules, $\langle P_L \rangle = 1$ if $L \geq 2$ and $f(\psi) = \delta(\cos\psi\text{-}1)$ (δ is Dirac's delta function). Intermediate distributions are characterized by their peculiar set of $\langle P_2 \rangle, \langle P_4 \rangle, \langle P_6 \rangle, \ldots$ However, only $\langle P_2 \rangle$ and $\langle P_4 \rangle$ can be determined from the experiment. Thus, the quest for $f(\psi)\sin(\psi)$ (probability density function, which takes into account the increase in the spherical crown surface of $\psi + d\psi$ as ψ increases) involves two steps: (1) $\langle P_2 \rangle$ and $\langle P_4 \rangle$ determination, and (2) finding an approximated function for $f(\psi)\sin(\psi)$ from $\langle P_2 \rangle$ and $\langle P_4 \rangle$ only. The most common realistic approximation combines the application of the maximum entropy method with the Lagrange multipliers method. In this approach, the approximated function is the one that maximizes the orientational entropy of the distribution, $S(f(\psi))$:

$$S(f(\psi)) = \int_0^\pi \ln(\psi)\sin(\psi) f(\psi)\,d\psi. \tag{14}$$

In other words, the resulting distribution is the broadest possible from all the universe of distributions having that particular $(\langle P_2 \rangle, \langle P_4 \rangle)$ pair (Castanho et al. 2003).

The combination of electronic absorption and emission phenomena in fluorescence spectroscopy, being both vectorial, enables obtaining $\langle P_2 \rangle$ and $\langle P_4 \rangle$ from which orientation distribution functions can be estimated (Castanho et al. 2003). Two classes of methodologies can be used, depending upon macroscopically ordered or disordered lipid membranes. In macroscopically aligned membranes information about the orientation of the transition dipolar moment can be obtained through the dependence of linearly polarized light absorption on the angle formed by light polarization and sample orientation (Castanho et al. 2003)—linear dichroism. Macroscopically aligned samples include vesicles deformed in a rotating flow (Brattwall et al. 2003) or supported multibilayers, which can be obtained by several methods such as the Langmuir–Blodgett (LB) technique (Roberts 1990; Schwartz 1997) or semi-dehydration of an aqueous lipid suspension under a gentle stream of nitrogen onto one side of a solid support (e.g. quartz slide) (Castanho et al. 2003).

When a quartz slide is covered with the macroscopically oriented sample its absorption variation (A_ω) with the measured angle (ω, the angle formed by the horizontal polarization direction relative to the normal of the bilayer; Fig. 7), using horizontally polarized light (h direction in Fig. 7) is given by

$$\frac{\sin(\omega)A_\omega}{A_{\omega=\pi/2}} = 1 + \frac{3\langle P_2 \rangle}{(1-\langle P_2 \rangle)n^2}\cos^2\,\omega \tag{15}$$

($\sin(\omega)$ and the relative refractive index, n, are introduced to account for experimental artefacts; Castanho et al. 2003). The term $\sin(\omega)A_\omega/A_{\omega=\pi/2}$ is the dichroic ratio and $\langle P_2 \rangle$ Eq. (12) regards the electronic absorption transition moment distribution relative to the normal of the membrane. If the molecular axis and the transition moment are parallel, the molecular distribution function has the same $\langle P_2 \rangle$.

The fluorescence emission linear dichroism methodology allows the calculation of the fourth rank order parameter ($\langle P_4 \rangle$). $\langle P_4 \rangle$ is calculated by means of a steady-state fluorescence spectroscopy having excitation and

emission in a 90° angle geometry, using polarized light (Kooyman and Levine 1981; Fig. 7). If the absorption and emission dipoles are parallel to the molecular symmetry axis, $\langle P_4 \rangle$ can be calculated from

$$\frac{GI_{vh}}{f'(\alpha)I_{vv}} = m \sin^2 \alpha + b', \quad G = \frac{I_{hv}}{I_{hh}} \tag{16}$$

where α is the angle between the emission direction and the membrane surface plane—Fig. 7, m and b' depend on both $\langle P_2 \rangle$ and $\langle P_4 \rangle$; G is a correcting factor that accounts for the different efficiency of the detecting system for parallel and perpendicular polarized light and $f'(\alpha)$ a correction factor for reflection (Kooyman and Levine 1981; Castanho et al. 2003). The subscripts in I_{ij} refer to the position of the excitation (i) or emission (j) polarizers in the lab frame (v, vertical; h, horizontal), as depicted in Fig. 7. $\langle P_2 \rangle$ is known from absorption experiments and $\langle P_4 \rangle$ can be obtained from the linear fit to the $GI_{vh}/(f'(\alpha).\ I_{vv})$ vs. $\sin^2 \alpha$ data, moreover $\langle P_4 \rangle$ can be calculated from both the slope and the intercept of $GI_{vh}/(f'(\alpha).\ I_{vv})$ vs. $\sin^2 \alpha$.

At variance with linear dichroism methodologies, fluorescence anisotropy measurements are based in photoselectivity. Therefore, the need for macroscopically oriented samples does not exist and lipid vesicles can be used. Fluorescence emission anisotropy, r, can de defined as

$$r = \frac{I_{\parallel} - I_{\perp}}{I_{\parallel} + 2I_{\perp}}, \tag{17}$$

where $I_{\parallel}$ and $I_{\perp}$ are the intensities of the polarization components parallel and perpendicular to the polarization of the excitation radiation, respectively. However the anisotropy in its functional form is

$$r = \frac{I_{vv} - GI_{vh}}{I_{vv} + 2GI_{vh}} \tag{18}$$

where the two subscripts in I are used to indicate the orientation of the excitation and emission polarizers, respectively (v, vertical; h, horizontal). The fluorescence anisotropy decay (anisotropy is followed in a nanosecond time scale, after pulse excitation of the fluorophores), $r(t)$, depends both on the molecular orientational order and dynamics during the fluorophore's excited state. At $t = 0$, $r(t)$, is only dependent on intrinsic spectroscopic characteristics of the fluorophore. Fluorophores that follow orientational distributions that are restricted (as most molecules inserted in lipid membranes) lead to limiting anisotropies, r_∞ ($r(t)$ in the limit $t \rightarrow \infty$), different from zero (i.e. depolarization is not complete). r_0 and r_∞ are related to the second rank order parameter ($\langle P_2 \rangle_r$) that can be obtained by the analysis of the decay through the following relation:

$$r_\infty = r_0 \langle P_2 \rangle_r^2. \tag{19}$$

Nevertheless this relation is only valid if (1) the transition moments are parallel to the symmetry axis of the molecule, and (2) if the orientational distribution function is the same in the excited and ground state. A more general equation would be (Johansson 1985):

$$r_\infty = r_0 \langle P_2 \rangle_r \langle P_2 \rangle_r^* \tag{20}$$

(* denotes an excited state parameter).

The $r(t)$ decay from r_0 to r_∞ is not only dependent on $\langle P_2 \rangle_r$ but also dependent on the fourth rank order parameter, $\langle P_4 \rangle_r$, and the rotational diffusion rate of the fluorophore around an axis perpendicular to the transition dipole, $D_\perp$. Zannoni et al. (1983) attained a

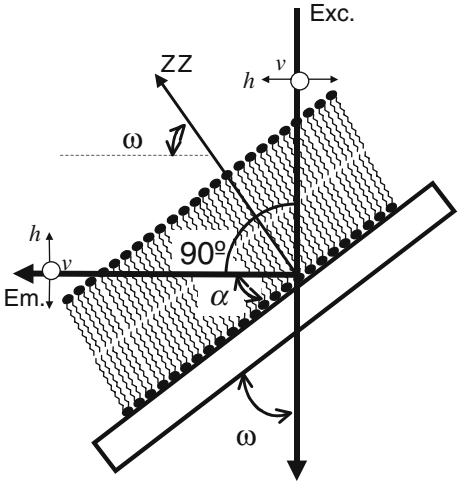

Fig. 7 Experimental setup for absorption and emission UV–Vis linear dichroism. In the absorption experiment ($\langle P_2 \rangle$ determination) the incident beam is horizontally polarized (h). In the emission experiment, fluorescence light is collected in a right angle geometry with both vertical and horizontal polarizations to determine $\langle P_4 \rangle$

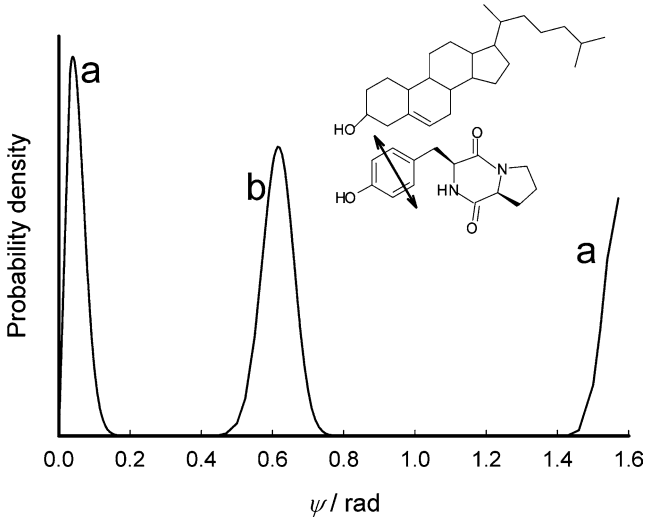

Fig. 8 Example of ligand orientation modulation by lipid membrane properties. The orientational probability density function of the maculosin (cyclo(L-tyrosyl-L-prolyl)) transition moment relative to the ^1L_b state (double arrow in the inserted structure) is shifted in the presence of cholesterol (curve a) relative to its absence (curve b) in POPC vesicles. This modulation is probably related to ring stacking between maculosin and sterol (structures inserted)

quantitative model for $r(t)$, assuming that $D_\perp$ is the same in the whole bilayer. Van der Meer et al. (1984) worked out simplified approximated equations, consisting of the sum of three exponentials plus a constant in which $\langle P_2\rangle_r$, $\langle P_4\rangle_r$ and $D_\perp$ can be obtained as fitting parameters in unoriented vesicles (e.g. Mitchell and Litman 1998).

UV–Vis linear dichroism methodologies have been applied in a large number of studies involving different classes of molecules such as membrane probes (Lopes et al. 2001; Lopes and Castanho 2004), polyene macrolide antibiotics (Lopes and Castanho 2002; Lopes et al. 2004a), multifunctional peptides (Lopes et al. 2004b, 2005) and DNA–ligand systems (Dafforn and Rodger 2005). The ability of cellular components to orient ligands has been demonstrated (Lopes et al. 2004b; Fig. 8). Recently fluorescence imaging of two-photon LD have been applied to study molecular orientation directly in cell membranes (Benninger et al. 2005).

Final remarks

(1) One of the most important roles attributed to membranes in the membrane catalysis model is the ability to optimize the conformation of the ligand, improving its docking to the receptor. This role was not given particular attention in this review because it was intensively explored in detail by the work of R. Schwyzer subsequent to the publication of the membrane catalysis model and extensive literature including reviews are available (Schwyzer 1991, 1992, 1995a,b). Nevertheless, the impact of membranes on the conformation of peptides remains a hot topic (e.g. Bombelli et al. 2004; Dhanasekaran et al. 2005) and the membrane-induced random/helix/β-sheet transition remains one of the most studied functionalities in membrane-active peptides (e.g. Wieprecht and Seelig 2002).

(2) The effect of ligand clustering may result from its high local concentration in the membranes. This effect may be selectively controlled by the membrane patched heterogeneity (Almeida et al. 2005). Clustering is believed to be important for some viral fusion processes, for instance (Chan and Kim 1998). However, the effect clustering may have on the interaction with receptors is not yet clear and well established. In theory patches may segregate or congregate ligands and receptors and thus have different effects.

Prospective conclusion

In the last section of the membrane catalysis model paper Sargent and Schwyzer (1986) made two sentences that proved to be premonitory:

(1) ''More detailed knowledge of the (...) lipid composition of the target cells will be necessary in elucidating [membrane receptor–ligand interactions]'' Recent work show that phospholipid headgroups may have very specific interactions with amino-acid side-chains in peptides leading to very peculiar effects, such as ''Arg magic'' (Sarai and Matile 2003).

(2) ''We hope that our ideas will stimulate new studies to elucidate molecular mechanisms governing receptor specificity, recognition, and stimulation''. Indeed their hope was fulfilled, at least for the 20 years that followed the publication of their model. Probably it will remain valid for years to come. The ability to perform structural studies in single molecules (Carrion-Vazquez et al. 1999; Reddy et al. 2004), including mechanical properties opened a new front. Conjugation of the modern approaches such as the ones presented in this paper with new fields in the future renews the interest of the membrane catalyst concept.

References

Adam G, Delbrück M (1968) Reduction of dimensionality in biological diffusion processes. In: Rich A, Davidson N (eds) Structural Chemistry and Molecular Biology. W.H. Freeman & Co., San Francisco, pp 198–215

Almeida RFM, Loura LMS, Prieto M (2005) Application of fluorescence to understand the interaction of peptides with binary lipid membranes. In: Geddes C, Lakowicz JR (eds) Reviews in Fluorescence 2005. Springer, Berlin Heidelberg New York, pp 271–323

Arkin IT, MacKenzie KR, Brijnger AT (1997) Site-Directed Dichroism As a Method for Obtaining Rotational and Orientational Constraints for Oriented Polymers. J Am Chem Soc 119:8973–8980

Axelrod D, Wang MD (1994) Reduction-of-dimensionality kinetics at reaction-limited cell surface receptors. Biophys J 66:588–600

Axelsen PH, Citra MJ (1996) Orientational order determination by internal reflection infrared spectroscopy. Prog Biophys Molec Biol 66:227–253

Baldo M, Grassi A, Raudino A (1991) Diffusion-controlled reactions among ligands and receptor clusters. Effects of competition for ligands. J Chem Phys 95:6734–6740

Bechinger B, Ruysschaert J-M, Goormaghtigh E (1999) Membrane helix orientation from linear dichroism of infrared attenuated total reflection spectra. Biophys J 76:552–563

Bechinger B, Aisenbrey C, Bertani P (2004) The alignment, structure and dynamics of membrane-associated polypeptides by solid-state NMR spectroscopy. Biochim Biophys Acta Biomemb 1666:190–204

Benninger RKP, Önfelt B, Davis DM, Neil M, French PMW (2005) Fluorescence imaging of two-photon linear dichroism: cholesterol depletion disrupts molecular orientation in cell membranes. Biophys J 88:609–622

Bombelli C, Borocci S, Lupi F, Mancini G, Mannina L, Segre AL, Viel S (2004) Chiral Recognition of Dipeptides in a Biomembrane Model. J Am Chem Soc 126:13354–13362

Brattwall CEB, Lincoln P, Norden B (2003) Orientation and Conformation of Cell-Penetrating Peptide Penetratin in Phospholipid Vesicle Membranes Determined by Polarized-Light Spectroscopy. J Am Chem Soc 125:14214–14215

Carrion-Vazquez M, Oberhauser AF, Fowler SB, Marszalek PE, Broedel SE, Clarke J, Fernandez JM (1999) Mechanical and chemical unfolding of a single protein: A comparison. Proc Nat Acad Sci USA 96:3694–3699

Castanho M, Prieto M (1992) Fluorescence study of the macrolide pentaene antibiotic filipin in aqueous solution and in a model system of membranes. Eur J Biochem 207:125–134

Castanho MARB, Lopes S, Fernandes M (2003) Using UV–Vis linear dichroism to study the orientation of molecular probes and biomolecules in lipid membranes. Spectroscopy Int J 17:377–398

Chan DC, Kim PS (1998) HIV entry and its inhibition. Cell 93:681–684

Chattopadhyay A, London E (1987) Parallax method for direct measurement of membrane penetration depth utilizing fluorescence quenching by spin-labeled phospholipids. Biochemistry 26:39–45

Cukier RI (1983) The effect of surface diffusion on surface reaction rates. J Chem Phys 79:2430–2435

Dafforn TMR, Rodger A (2005) Linear dichroism of biomolecules: which way is up?. Curr Opin Struc Biol 14:541–546

DeLisi C (1980) The biophysics of ligand–receptor interactions. Q Rev Biophys 13:201–230

Dhanasekaran M, Palian MM, Alves I, Yeomans L, Keyari CM, Davis P, Bilsky EJ, Egleton RD, Yamamura HI, Jacobsen NE, Tollin G, Hruby VJ, Porreca F, Polt R (2005) Glycopeptides Related to -Endorphin Adopt Helical Amphipathic Conformations in the Presence of Lipid Bilayers. J Am Chem Soc 127:5435–5448

Erickson J, Goldstein B, Holowka D, Baird B (1987) The effect of receptor density on the forward rate constant for binding of ligands to cell surface receptors. Biophys J 52:657–663

Fernandes MX, García de la Torre J, Castanho MARB (2002) Joint determination by Brownian dynamics and fluorescence quenching of the in-depth location profile of biomolecules in membranes. Analytical Biochemistry 307:1–12

Fung BM (2003) New angles for NMR studies of biological molecules. Biophys J 85:3429–3430

Gershon ND, Porter KR, Trus BL (1985) The cytoplasmic matrix: its volume and surface area and the diffusion of molecules through it. Proc Natl Acad Sci 82:5030–5034

Goormaghtigh E, Raussens V, Ruysschaert J-M (1999) Attenuated total reflection infrared spectroscopy of proteins and lipids in biological membranes. Biochim Biophys Acta 1422:105–185

Haugh JM, Lauffenburger DA (1997) Physical modulation of intracellular signalling processes by locational regulation. Biophys J 72:2014–2031

Henriques S, Castanho M (2004) Consequences of Nonlytic Membrane Perturbation to the Translocation of the Cell Penetrating Peptide Pep-1 in Lipidic Vesicles. Biochemistry 43:9716–9724

Henriques S, Castanho M (2005) Environmental factors that enhance the action of the cell penetrating peptide pep-1. A spectroscopic study using lipidic vesicles. Biochim Biophys Acta Biomemb 1669:75–86

Heyse S, Stora T, Schmid E, Lakey JH, Vogel H (1998) Emerging techniques for investigating molecular interactions at lipid membranes. Biochim Biophys Acta 85507:319–338

Høyrup P, Davidsen J, Jørgensen K (2001) Lipid membrane partitioning of lysolipids and fatty acids: effects of membrane phase structure and detergent chain length. J Phys Chem B 105:2649– 2657

Johansson LB-Å (1985) Order parameters of fluorophores in ground and excited states. Probe molecules in a lyotropic liquid crystal. Chem Phys Lett 118:516–521

Kooyman RPH, Levine YK (1981) Measurement of second and fourth rank order parameters by fluorescence polarization experiments in a lipid membrane system. Chem Phys 60:317–326

Ladokhin AS (1997) Distribution analysis of depth-dependent fluorescence quenching in membranes. Methods Enzymol 278:462–473

Lopes S, Castanho MARB (2002) Revealing the Orientation of Nystatin and Amphotericin B in Lipidic Multilayers by UV–Vis Linear Dichroism. J Phys Chem B 106:7278–7282

Lopes S, Castanho MARB (2004) Does Aliphatic Chain Length Influence Carbocyanines' Orientation in Supported Lipid Multilayers?. Journal of Fluorescence 14:281–287

Lopes SCDN, Castanho MARB (2005) Overview of Common Spectroscopic Methods to Determine the Orientation/Alignment of Membrane Probes and Drugs in Lipidic Bilayers. Curr Org Chemistry 9:889–898

Lopes S, Fernandes MX, Prieto M, Castanho MARB (2001) Orientational Order of the Polyene Fatty Acid Membrane Probe trans-Parinaric Acid in Langmuir-Blodgett Multilayer Films. J Phys Chem B 105:562–568

Lopes S, Fedorov A, Castanho M (2004) Cholesterol modulates maculosin's orientation in model systems of biological membranes. Relevance towards putative molecular recognition. Steroids 69:825–830

Lopes SCDN, Goormaghtigh E, Costa Cabral BJ, Castanho MARB (2004) Filipin Orientation Revealed by Linear Dichroism. Implication for a Model of Action. J Am Chem Soc 126:5396–5402

Lopes SCDN, Fedorov A, Castanho MARB (2005) Lipidic Membranes Are Potential "Catalysts" in the Ligand Activity of the Multifunctional Pentapeptide Neokyotorphin. Chem Bio Chem 6:697–702

Martins J, Melo E, Naqvi KR (2004) Reappraisal of four different approaches for finding the mean reaction time in the multi-trap variant of the Adam-Delbrück problem. J Chem Phys 120:9390–9393

Mitchell DC, Litman BJ (1998) Molecular order and dynamics in bilayers consisting of highly polyunsaturated phospholipids. Biophys J 74:879–891

Murray D, Arbuzova A, Honig B, McLaughlin S (2002) The role of electrostatic and nonpolar interactions in the association of peripheral proteins with membranes. In: Simon SA, McIntosh TJ (eds) Peptide-lipid interactions. Academic Press, San Diego, pp 277–307

Reddy CVG, Malinowska K, Menhart N, Wang R (2004) Identification of TrkA on living PC12 cells by atomic force microscopy. Biochim Biophys Acta Biomemb 1667:15–25

Roberts GG (1990) Langmuir Blodgett films. Plenum Press, New York

Santos N, Prieto M, Castanho M (2003) Quantifying molecular partition into model systems of biomembranes: an emphasis on optical spectroscopic methods. Biochim Biophys Acta Biomemb 1612:123– 135

Sarai N, Matile S (2003) Anion-mediated transfer of polyarginine across liquid and bilayer membranes. J Am Chem Soc 125:14348–14356

Sargent DF, Schwyzer R (1986) Membrane lipid phase as catalyst for peptide-receptor interactions. Proc Natl Acad Sci USA 83:5774–5778

Schwartz DK (1997) Langmuir-Blodgett film structure. Surf Sci Rep 27:245–334

Schwyzer R (1991) New principles in QSAR: membrane requirements. J Recept Res 11:45–47

Schwyzer R (1992) How do peptides interact with lipid membranes and how does this affect their biological affinity?. Braz J Med Biol Res 25:1077–1089

Schwyzer R (1995a) 100 years lock-and-key concept: are peptides keys shaped and guided to their receptors by the target cell membrane?. Biopolymers 37:5–16

Schwyzer R (1995b) In search of the 'bio-active conformation'–is it induced by the target cell membrane?. J Mol Recognit 8:3–8

Tatulian SA (2003) Attenuated total reflection Fourier transform infrared spectroscopy: a method of choice for studying membrane proteins and lipids. Biochemistry 42:11898–11907

Van der Meer W, Pottel H, Herrennan W, Ameloot M, Hendrickx M, Schröder H (1984) Effect of orientational order on the decay of the fluorescence anisotropy in membrane suspensions. A new approximate solution of the rotational diffusion equation. Biophys J 46:515–523

Veiga S, Henriques S, Santos N, Castanho M (2004a) Putative role of membranes in the HIV fusion inhibitor enfuvirtide mode of action at the molecular level. Biochem J 377:107–110

Veiga S, Santos N, Loura L, Fedorov A, Castanho M (2004b) HIV Fusion Inhibitor Peptide T-1249 Is Able To Insert or Adsorb to Lipidic Bilayers. Putative Correlation with Improved Efficiency. J Am Chem Soc 126:14758–14763

Vigano C, Manciu L, Buyse F, Goormaghtigh E, Ruysschaert J-M (2000) Attenuated total reflection IR spectroscopy as a tool to investigate the structure, orientation and tertiary structure changes in peptides and membrane proteins. Biopolymers 55:373–380

Wasniewski CM, Parkanzky PD, Bodner ML, Weliky DP (2004) Solid-state nuclear magnetic resonance studies of HIV and influenza fusion peptide orientations in membrane bilayers using stacked glass plate samples. Chem Phys Lipids 132:89–100

Wieprecht T, Seelig J (2002) Isothermal titration calorimetry for studying interactions between peptides and lipid membranes. In: Simon SA, McIntosh TJ (eds) Peptide-lipid interactions. Academic Press, San Diego, pp 31–56

Zandomeneghi G, Tomaselli M, van Beek JD, Meier BH (2001) Manipulation of the Director in Bicellar Mesophases by Sample Spinning: A New Tool for NMR Spectroscopy. J Am Chem Soc 123:910–913

Zannoni C, Arcioni A, Cavatorta P (1983) Fluorescence depolarization in liquid crystals and membrane bilayers. Chem Phys Lipids 32:179–250